J|A|C|S
ARTICLES

Published on Web 07/28/2009

Electrostatic Charging of Hydrophilic Particles Due to Water Adsorption

Rubia F. Gouveia and Fernando Galembeck*

Institute of Chemistry, University of Campinas-UNICAMP, P.O. Box 6154, 13083-970 Campinas, SP, Brazil

Received January 28, 2009; E-mail: fernagal@iqm.unicamp.br

Abstract: Kelvin force microscopy measurements on films of noncrystalline silica and aluminum phosphate particles reveal complex electrostatic potential patterns that change irreversibly as the relative humidity changes within an electrically shielded and grounded environment. Potential adjacent to the particle surfaces is always negative and potential gradients in excess of ±10 MV/m are found parallel to the film surface. These results verify the following hypothesis: the atmosphere is a source and sink of electrostatic charges in dielectrics, due to the partition of OH^- and H^+ ions associated to water adsorption. Neither contact, tribochemical or electrochemical ion or electron injection are needed to change the charge state of the noncrystalline hydrophilic solids used in this work.

Introduction

Electrostatic charging is familiar to most persons, but knowledge on this topic is still rather empiric,[1−3] mainly because fundamental ideas on the structure of matter are not well-connected to the phenomenology of insulator charging.[4−12] The present work shows that water adsorption and desorption modify charge status of solids, within a shielded environment and thus without any explicit electrical input.

Evidence for ion participation in the formation of charge patterns in some latex particles and silica particles and films[13−17] is increasing. Electret patterning on some surfaces[18−21] has been obtained based on charge accumulation due to ion transfer at surfaces, following ion partition events or electrochemical discharge at neighboring electrodes.[16,17] On the other hand, recent evidence for tribochemical formation of free electrons in polytetrafluoroethylene surfaces has also been described.[22]

The insufficiency of current knowledge on electrostatic charge mechanisms is not restricted only to the materials area: current geophysical research has not yet disclosed effective models for atmospheric cloud electrification,[23] but there is growing evidence on the ability of water to accumulate excess charge.[24]

This situation leaves room for hazards and accidents associated to uncontrolled electrostatic discharges that take a heavy toll in lives and property throughout the world, every year. Moreover, lack of knowledge on mechanisms for electrostatic charge accumulation and dissipation also prevents the collection and use of energy from the atmospheric electricity that is instead a source of problems and serious accidents.

The role of atmospheric water is now generally acknowledged and it was already evidenced in Schrödinger's doctoral thesis that also showed the importance of solid surface status for electrostatic charge dissipation.[25] Current discussions on the effect of humidity on electrostatic behavior are usually concentrated on its contribution to increase surface conductance and many substances used as antistatic agents, like nonionic surfactants, are believed to perform by increasing surface conductance associated to increased water adsorption.

Recent work from this group showed that many experimental results can be understood following a simple but new hypothesis:[16,17,26] atmospheric water is a source and sink of charges for dielectrics and these are exchanged with the solid

(1) Schein, L. B. *Science* **2007**, *316*, 1572.
(2) Bailey, A. G. *J. Electrost.* **2001**, *51*, 82.
(3) Castle, G. S. P. *J. Electrost.* **1997**, *40*, 13.
(4) Németh, E.; Albrecht, V.; Schubert, G.; Simon, F. *J. Electrost.* **2003**, *58*, 3.
(5) Davidson, J. L.; Williams, T. J.; Bailey, A. G.; Hearn, G. L. *J. Electrost.* **2001**, *51*, 374.
(6) Chen, G.; Tanaka, Y.; Takada, T.; Zhong, L. *IEEE Trans. Dielectr. Electr. Insul.* **2004**, *11*, 113.
(7) Hogue, M. D.; Buhler, C. R.; Calle, C. I.; Matsuyama, T.; Luo, W.; Groop, E. E. *J. Electrost.* **2004**, *61*, 259.
(8) Chen, G.; Tay, T. Y. G.; Davies, A. E.; Tanaka, Y.; Takada, T. *IEEE Trans. Dielectr. Electr. Insul.* **2001**, *8*, 867.
(9) Bigarré, J.; Hourquebie, P. *J. Appl. Phys.* **1999**, *85*, 7443.
(10) Duff, N.; Lacks, D. J. *J. Electrost.* **2008**, *66*, 51.
(11) Choi, K. S.; Yamaguma, M.; Ohsawa, A. *Jpn. J. Appl. Phys.* **2007**, *46*, 7861.
(12) Park, A. A.; Fan, L. S. *Chem. Eng. Sci.* **2007**, *62*, 371.
(13) Galembeck, A.; Costa, C. A. R.; Silva, M. C. V. M.; Souza, E. F.; Galembeck, F. *Polymer* **2001**, *42*, 4845.
(14) Rezende, C. A.; Gouveia, R. F.; da Silva, M. A.; Galembeck, F. *J. Phys.: Condens. Matter* **2009**, *21*, 263002.
(15) Braga, M.; Costa, C. A. R.; Leite, C. A. P.; Galembeck, F. *J. Phys. Chem. B* **2001**, *105*, 3005.
(16) Gouveia, R. F.; Costa, C. A. R.; Galembeck, F. *J. Phys. Chem. B* **2005**, *109*, 4631.
(17) Gouveia, R. F.; Costa, C. A. R.; Galembeck, F. *J. Phys. Chem. C* **2008**, *112*, 17193.
(18) McCarty, L. S.; Whitesides, G. M. *Angew. Chem., Int. Ed.* **2008**, *47*, 2188.
(19) Jacobs, H. O.; Whitesides, G. M. *Science* **2001**, *291*, 1763.
(20) McCarty, L. S.; Winkleman, A.; Whitesides, G. M. *J. Am. Chem. Soc.* **2007**, *129*, 4075.
(21) McCarty, L. S.; Winkleman, A.; Whitesides, G. M. *Angew. Chem., Int. Ed.* **2007**, *46*, 206.
(22) Liu, C.; Bard, A. J. *Nat. Mater.* **2008**, *7*, 505.
(23) Helsdon, J. H., Jr.; Gattaleeradapan, S.; Farley, R. D.; Waits, C. C. *J. Geophys. Res.* **2002**, *107*, 4630.
(24) Ovchinnikova, K.; Pollack, G. H. *Langmuir* **2009**, *25*, 542.
(25) Schrödinger, E. Ph.D. Thesis, University of Vienna, Vienna, 1910.

surfaces during the water vapor adsorption and desorption events. Thus, the rates of charge dissipation and accumulation are dependent on adsorption−desorption rates that in turn depend on the nature of the surface, on the atmospheric relative humidity, and temperature.

Verification of this hypothesis requires extensive testing in various systems. A conceivable test is to measure electrostatic potential distribution across the surface of different solids under different values of relative humidity, observing the resulting variations in local electrostatic potentials. These experiments were done on glassy aluminum phosphate and Stöber silica particle films and their results are reported in the present work.

Experimental Section

Aluminum Phosphate Particles. Amorphous aluminum phosphate is a developmental product supplied by Bunge.[27−29] Chemical composition is $(Al(OH)_{0.7}Na_{0.7}(PO_4)\cdot 1.7H_2O)$, particle size in aqueous dispersion is 293 nm, and zeta potential is −25.2 mV both measured at pH 7.8 by acoustic and electroacoustic techniques, respectively, using a Dispersion Technology Spectrometer DT 1200 instrument.

Stöber Silica Particles. Silica particles are prepared by the method of Stöber et al.[30,31] Reagent-grade tetraethoxysilane (TEOS; Merck), absolute ethanol (Merck) as the solvent, and ammonium hydroxide (Synth) were used. The effective silica particle diameter and zeta potential by photon correlation spectroscopy (PCS) are 169 nm and −65 mV, respectively, using a ZetaPlus instrument (Brookhaven Instruments).

Kelvin Force Microscopy (KFM). Aluminum phosphate dispersions droplets were allowed to dry on top of freshly cleaved mica surfaces and Stöber silica dispersions were dried on silicon wafers substrates. The samples were dried at 23−25 °C and relative humidity 55%, prior to mounting on the scanning probe microscope sample holder.

Electrostatic patterns in the submicrometer range were obtained by electric potential (Kelvin) scanning probe microscopy (KFM or SEPM),[32] using Shimadzu WET-SPM 9600J3 instrument. The microscope is fully contained within an environmental chamber that allows control of ambient pressure, temperature, relative humidity, and atmosphere composition.

The KFM technique uses the standard noncontact AFM setup, but the sample is scanned with Pt-coated Si tips with a 20 nm nominal radius.

An AC signal is fed 10−20 kHz below the frequency of the normal AFM oscillator, which matches the natural frequency of mechanical oscillation of the cantilever-tip system (40−70 kHz). The principle is analogous to the Kelvin method,[33] except that forces are measured instead of current. The image is built using the DC voltage fed to the tip, at every pixel, thus detecting electric potential gradients throughout the scanned area.

Results

Kelvin micrographs from aluminum phosphate particle layers are presented with standard noncontact images, in Figure 1. They were acquired initially after equilibrating for 90 min at 30% RH. Relative humidity was then changed to 50%, then to 70% and back to 30% RH.

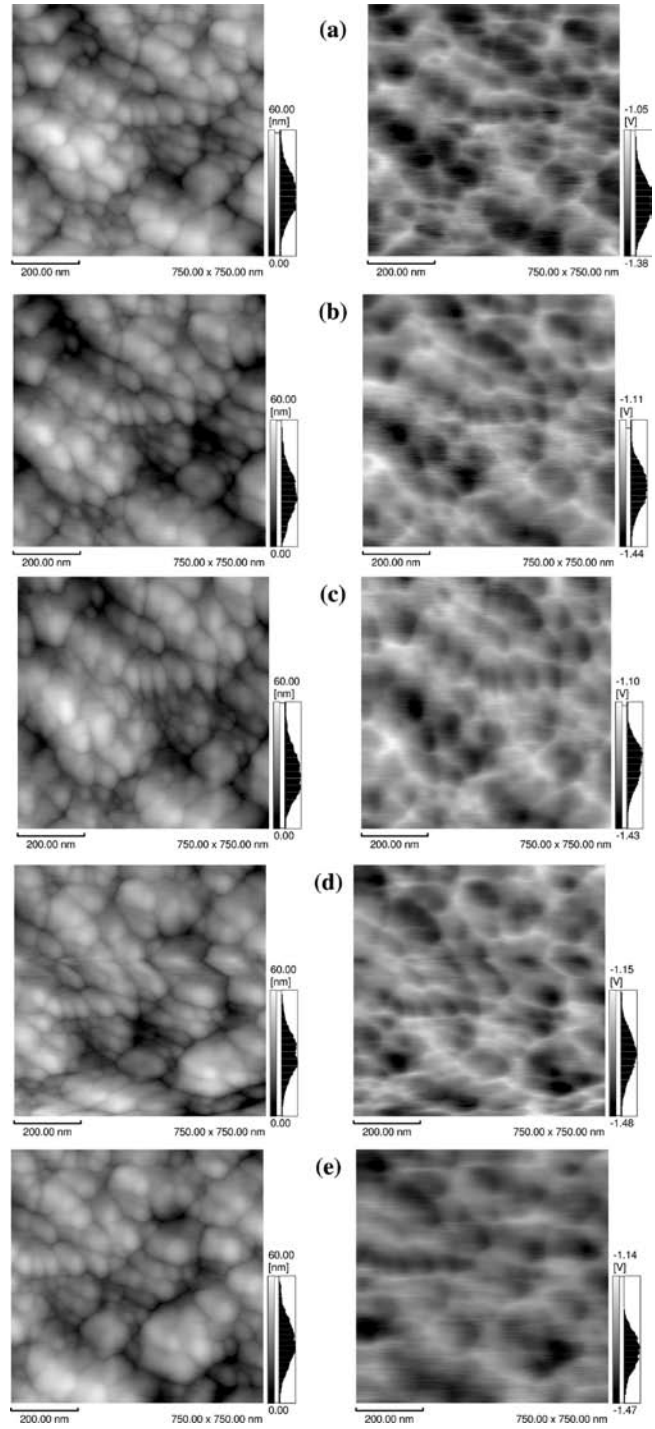

Figure 1. AFM (left) and KFM (right) images from aluminum phosphate particle films. Successive changes in the relative humidity were made prior to image acquisition: (a) 30% RH (after equilibrating for 90 min); (b) 50% RH (after equilibrating for 90 min); (c) 70% RH (after equilibrating for 90 min); (d) back to 30% RH (image acquisition started immediately); and (e) 30% RH (after equilibrating for 90 min).

All images show some common features. First, the overall sample potential is always negative, at any point, meaning that the particles carry an excess negative charge that is not surprising, considering that particles zeta potential is negative, under water at neutral pH. However, the average potential increases as the relative humidity is increased and it becomes

(26) Soares, L. C.; Bertazzo, S.; Burgo, T. A. L.; Baldim, V.; Galembeck, F. *J. Braz. Chem. Soc.* **2008**, *19*, 277.
(27) Rosseto, R.; Santos, A. C. M. A.; Galembeck, F. *J. Braz. Chem. Soc.* **2006**, *17*, 1412.
(28) Galembeck, F.; Silva, M. C. V. M.; Rosseto, R. *Química Nova* **2007**, *3*, 745.
(29) De Brito, J.; Galembeck, F.; Rosseto, R.; Dos Santos, A. C. M. A. PCT Int. Appl. WO 2008/017135, 2008.
(30) Stöber, W.; Fink, A.; Bohn, E. *J. Colloid Interface Sci.* **1968**, *26*, 62.
(31) Leite, C. A. P.; de Souza, E. F.; Galembeck, F. *J. Braz. Chem. Soc.* **2001**, *12*, 519.
(32) Galembeck, F.; Costa, C. A. R. *Encyclopedia of Surface and Colloid Science*; Dekker Encyclopedias: New York, 2006; p 1874.
(33) Nonnenmacher, M.; O' Boyle, M. P.; Wickramasinghe, H. K. *Appl. Phys. Lett.* **1991**, *58*, 2921.

more negative again when the humidity is decreased, showing that water desorption increases the overall sample charge even within a grounded environment. This can be interpreted assuming that ion partitioning is concurrent to adsorption−desorption events: desorbed water molecules and clusters carry excess positive charge, even though the overall sample potential is negative and pointing to a role of specific interactions between water ions and the ions in the aluminum phosphate sample.

The potential measurements show that the particles carry excess negative charge. The authors recently showed that calculated potentials in the vicinity of an overall neutral virtual particle can be only positive or negative, but at much larger distances than the 10 nm used in KFM.[14]

Potential profiles line-scanned across the sample are shown in Figure 2. Steep potential change between neighboring points show that electroneutrality is not observed even at this scale size, challenging currently accepted ideas on electroneutrality.[18]

Potential values for successive measurements for many sample points in Figure 1 are presented in Figure 3. There is a pattern for potential change: the local potential increases (becomes less negative) when humidity is increased to decrease later when the humidity decreases, parallel to the observed overall sample behavior. The potential measurement at 30% RH is not reversible, showing that irreversible transformations took place within the sample, when this was transferred to a more humid environment and back.

From the line-scans in Figure 2, potential gradients can be calculated at any position in the sample. Potential derivatives with distance yield the field component across the *x*-axis and their values are presented in Figure 4. Large electric fields are parallel to the surface with spikes in excess of ±4 MV/m in a range where air can already start to break down.[34] Even larger potential gradients may have been formed during particle dispersion drying, but these led to discharge and the ions then formed deposited on the sites with larger charge excess.

The potential gradient plots for the sample under 30% RH both before and after the sample was subjected to higher humidity are clearly different showing that cycling through high humidity decreased local charge excesses, in an irreversible way. Weight gain and loss are reversible according to data in Supporting Information (Table S1). There are at least two possible mechanisms to explain this behavior: increased ion mobility within the particles at higher humidity and more intense adsorption−desorption of water ions at the spots with extreme charge excess, partially neutralizing them. The first hypothesis is not sustained by the following observation: at 70% RH, large gradients are still observed, but these are abated when humidity is lowered back to 30% (Figure 4b).

The potential gradients also reveal that the surfaces are electrically rough independently of the amount of absorbed water. This means they are formed by fixed charges, which strongly rules out the existence of percolating surface liquid films, because aqueous films containing ions are equipotential, as any other conductive surface.

A similar set of experiments was done using Stöber silica particles, producing the AFM and KFM micrographs presented in Figure 5. Silica surface is always negative, the same as aluminum phosphate. Growth of the upper end of the AFM histograms reveals that particles are swollen but to a limited extent, while the potential histograms from the KFM images show an overall displacement toward negative potentials under higher humidity that is largely reversed when humidity is reduced to the original value. Thus, silica shows more reversible behavior than aluminum phosphate.

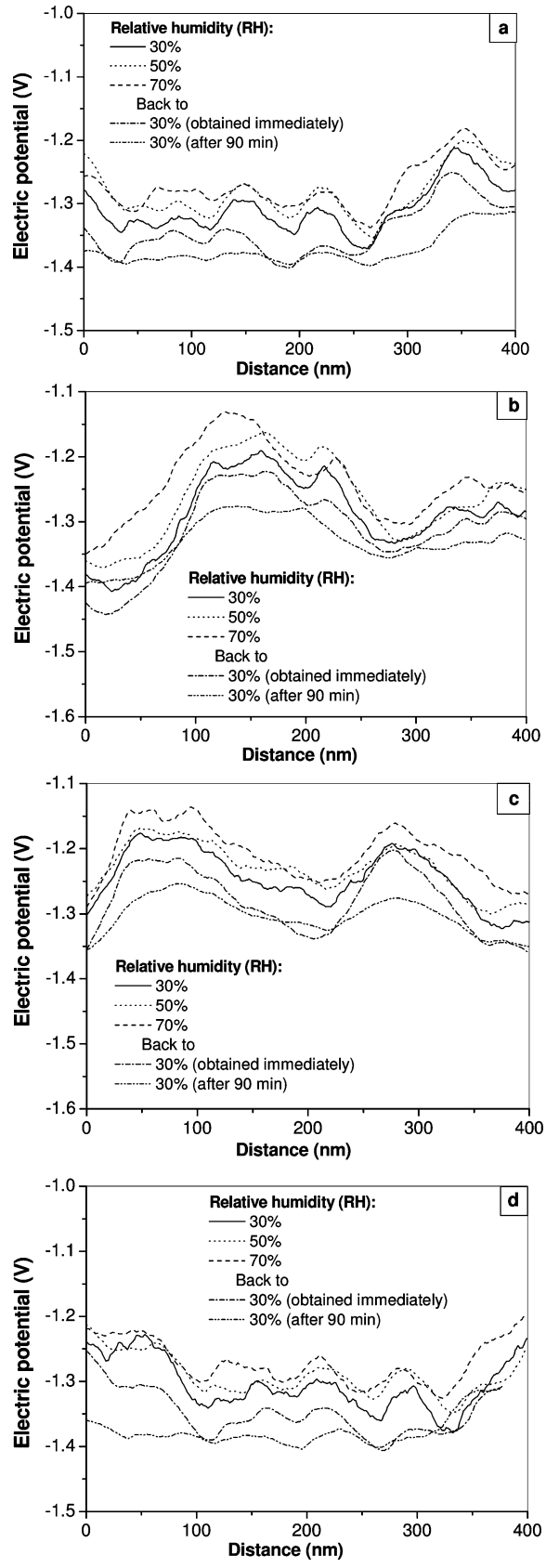

Figure 2. Line-scans from the five consecutive KFM images from aluminum phosphate particles.

(34) Hu, Z.; Seggern, H. *J. Appl. Phys.* **2005**, *98*, 014108.

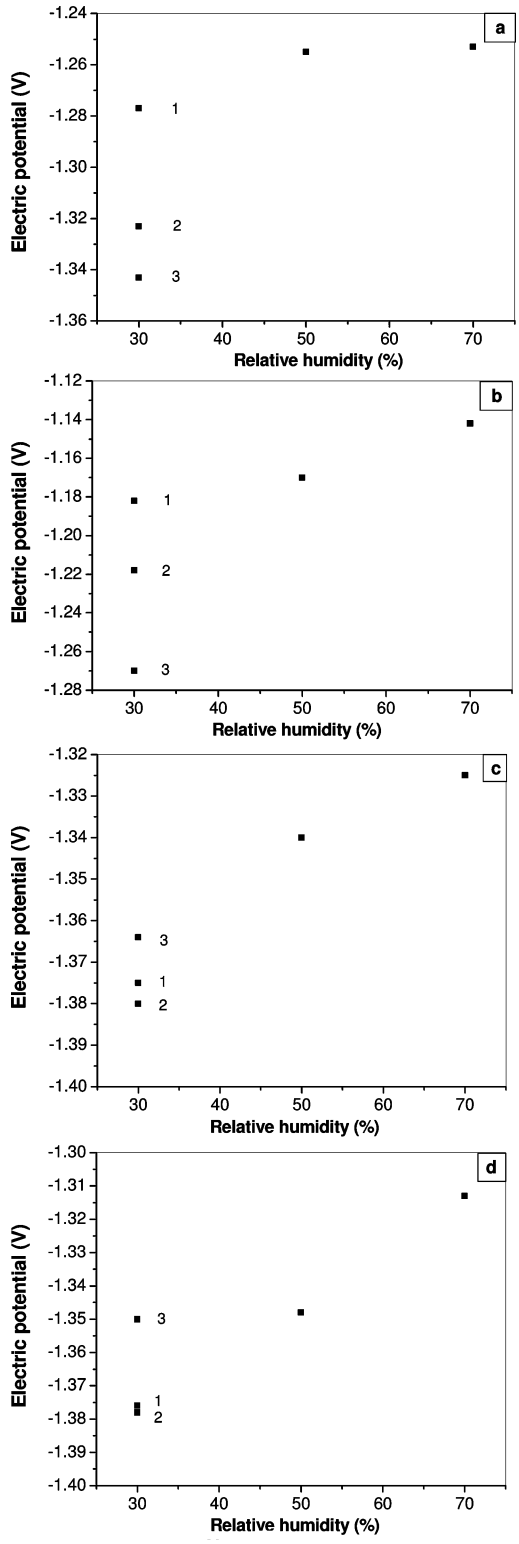

Figure 3. Electric potential values from successive measurements for some sample points in Figure 1. Numbers drawn in the graphs refer to (1) 30% RH (initial measurements), (2) back to 30% RH (acquired immediately after change RH), and (3) 30% RH (after equilibrating for 90 min).

This can be better seen in Figures 6 and 7. The first shows electric potential along a randomly chosen line, as the humidity changes, and the latter shows that electrostatic potential becomes more negative at higher humidity but moves back to zero under 30% RH.

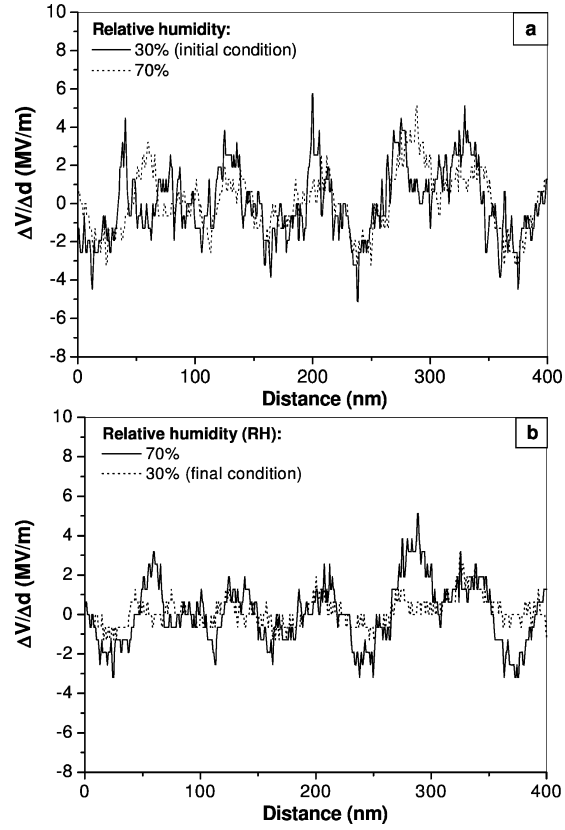

Figure 4. Electric potential gradients calculated as a function of the sample from aluminum phosphate particles after equilibrating for 90 min. (a) 30% RH (solid line, initial condition) and 70% RH (dot line). (b) 70% RH (solid line) and 30% RH (dot line, final condition).

Potential gradients measured along silica surface are also dependent on relative humidity and the extreme values are larger than those observed for aluminum phosphate (Figure 8).

Discussion

Surface potential of the amorphous hydrophilic particles used in this work change without any electrochemical or inductive input, just by changing humidity and thus absorbing and desorbing water. Patterns of potential change are different for the two substances used: silica surface becomes more negative at higher humidity, while aluminum phosphate becomes more positive.

Surface potential gradients decrease upon cycling the samples through high and low humidity, showing irreversible changes and suggesting that these can continue under further cycling. The structural changes that account for the measured potential variations are triggered by water adsorption, either neutral water or water ions. Since these samples swell under water, initial changes take place at the surface of the particles, but they should be followed by water migration to and from the particle interior, what accounts for the slow potential changes detected when the sample is equilibrated at 30% RH under longer times.

Since the aluminum phosphate and silica samples used in this work are simple solids representative of many noncrystalline solids that are commonly found in a large number of practical applications and also in the environment, the present results can probably be generalized for many other inorganic compounds. If this is further verified, atmospheric water should be acknowledged as a charge reservoir for insulators. This is quite different from the current view that assigns to water an important but

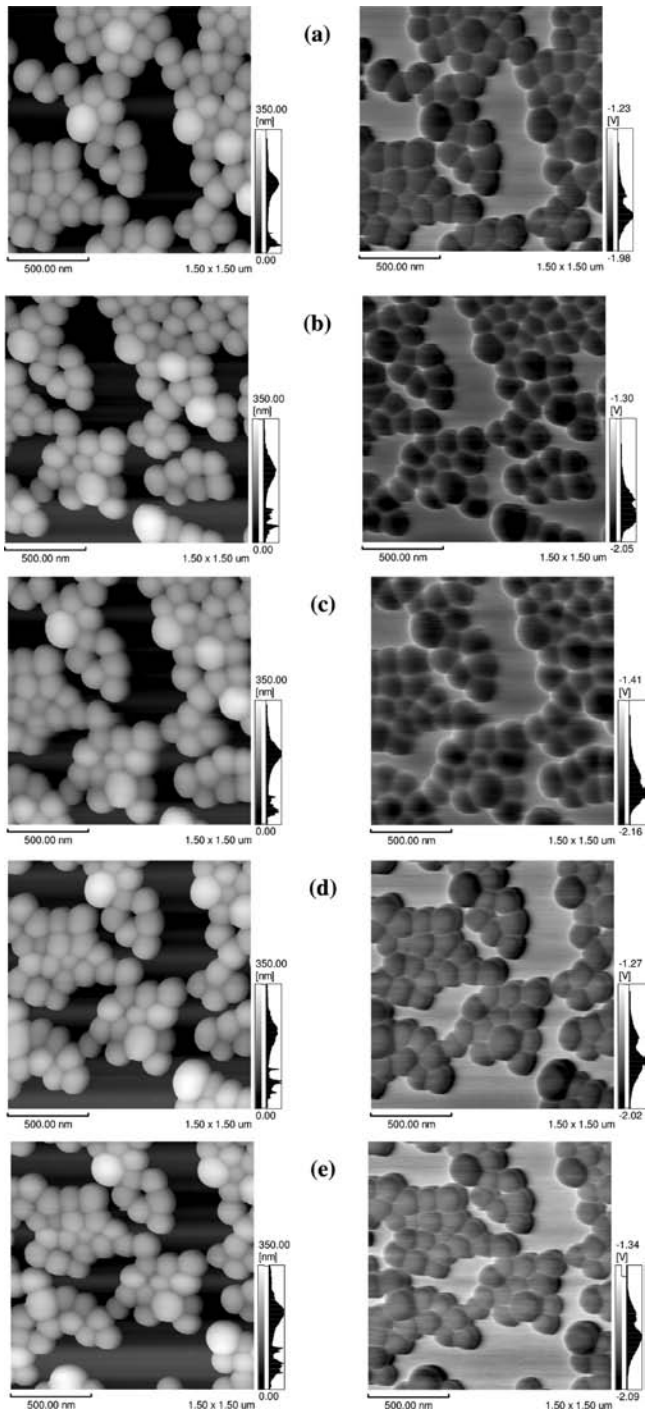

Figure 5. AFM (left) and KFM (right) images from Stöber silica particle films. Successive changes in the relative humidity were made prior to image acquisition: (a) 30% RH (after equilibrating for 90 min); (b) 50% RH (after equilibrating for 90 min); (c) 70% RH (after equilibrating for 90 min); (d) back to 30% RH (image acquisition started immediately); and (e) 30% RH (after equilibrating for 90 min).

passive role in insulator electrification, contributing to charge dissipation by increasing interfacial and bulk conductance of contacting phases. According to the present results, water has an active role and humid air is an agent for charge build-up, while keeping its well-established role in increasing charge conduction. The prevalence of one or another contribution will largely depend on the morphology and composition of the surface aqueous films: percolating films should form large equipotential surface patches, while large potential gradients can

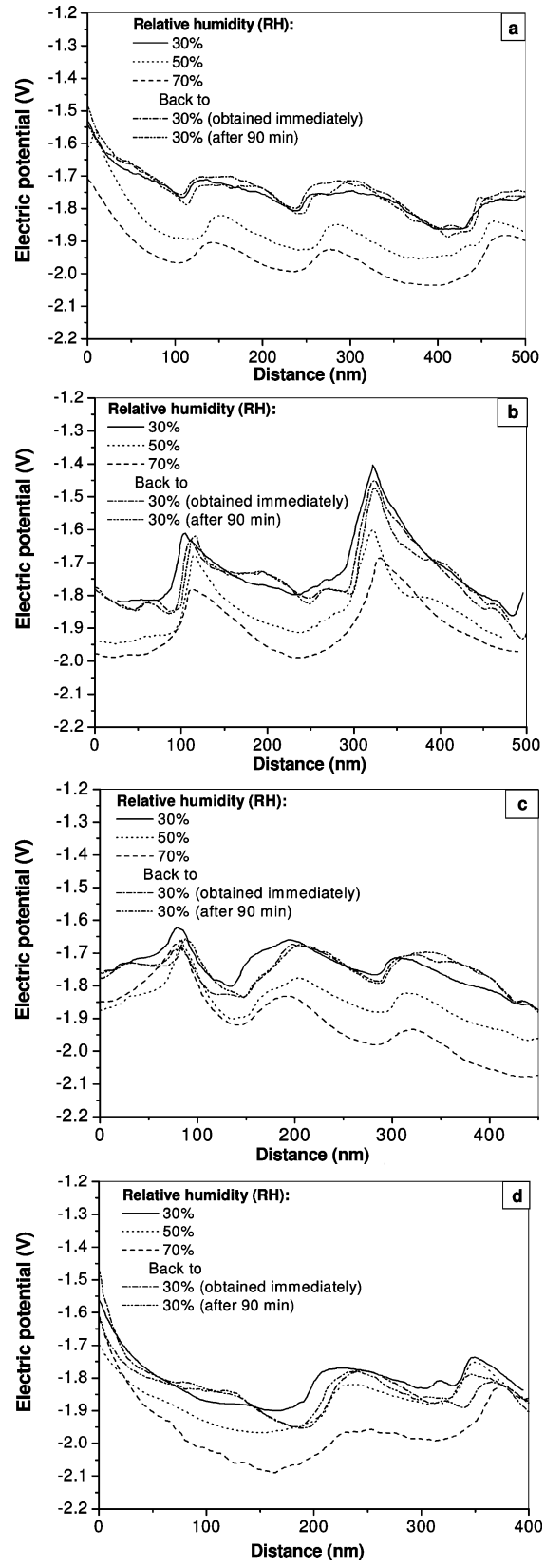

Figure 6. Line-scans from the five consecutive KFM images from Stöber silica particles.

only be due to sharp and stable charge concentration gradients that cannot exist within continuous conducting films. Conflicting outcomes of these two effects of surface water are certainly a source of the well-known difficulties in making reproducible electrostatic experiments.

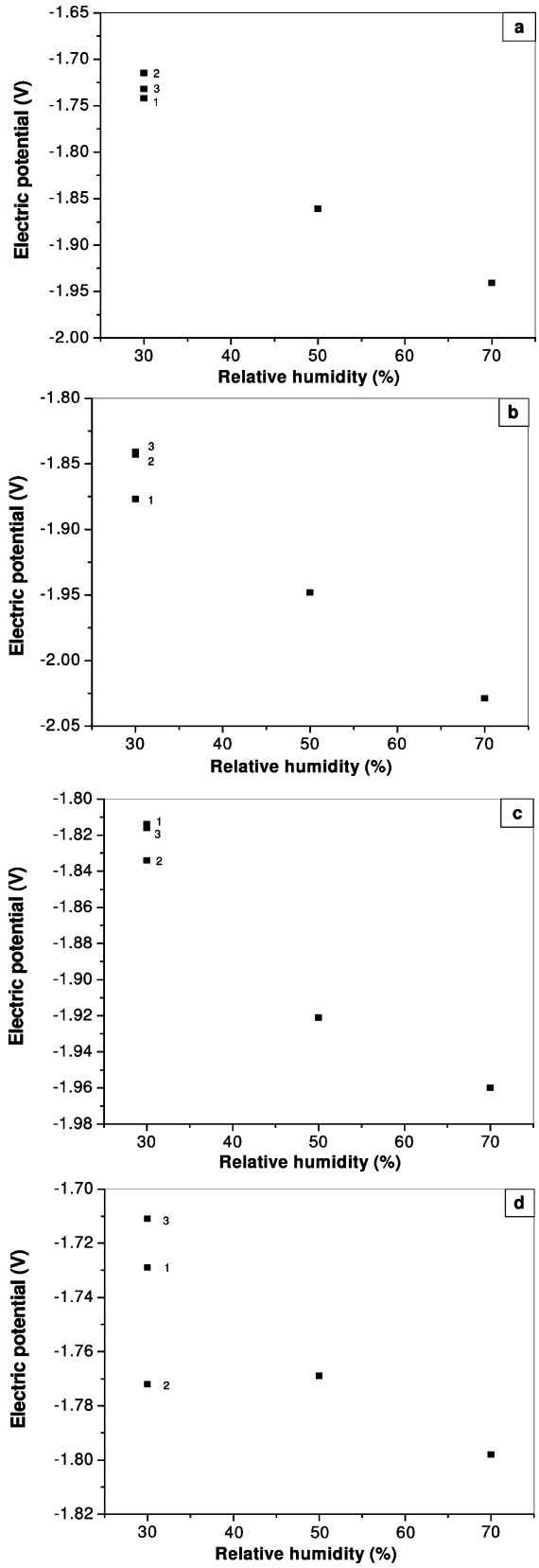

Figure 7. Electric potential values from successive measurements for some sample points in Figure 5. Numbers drawn in the graphs refer to (1) 30% RH (initial measurements), (2) back to 30% RH (acquired immediately after change RH), and (3) 30% RH (after equilibrating for 90 min).

Finally, charge exchange between solids and the atmosphere should depend on the local electric potential, following the

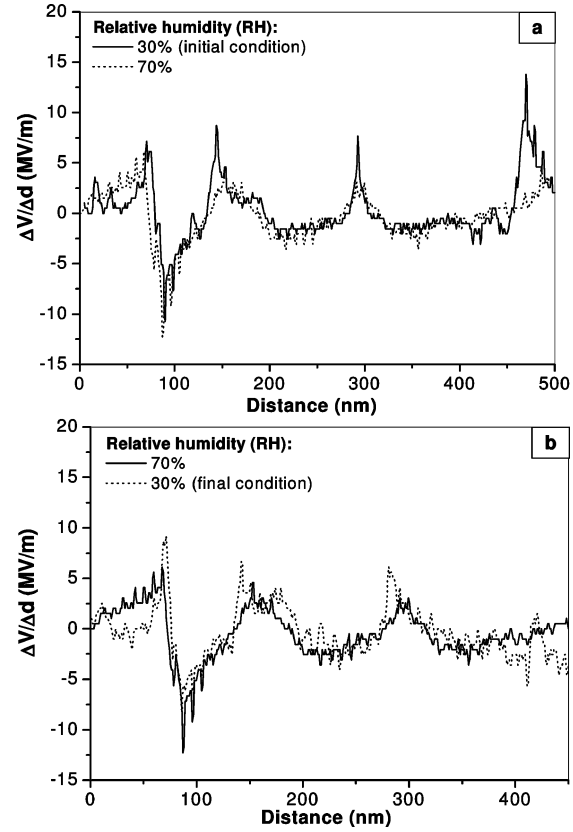

Figure 8. Electric potential gradients calculated as a function of the sample position for Stöber silica particles after equilibrating for 90 min. (a) 30% RH (solid line, initial condition) and 70% RH (dot line). (b) 70% RH (solid line) and 30% RH (dot line, final condition).

condition for electrochemical potential under equilibrium.[14,16,17,26] In the present work, samples were fully shielded within grounded containers and, thus, protected from external potentials. However, in the open air, this condition is not met and significant electrostatic potential gradients are found throughout, creating one additional factor for making insulator charging very complex.

Conclusion

The electrostatic potential measured along the surface of noncrystalline silica and aluminum phosphate changes with relative humidity, within a grounded environment. This can be interpreted assuming that ion partitioning is concurrent to adsorption−desorption events: desorbed water molecules and clusters carry excess positive charge in aluminum phosphate and negative charge in silica, even though the overall sample potential is negative. Thus, specific interactions between water ions and the ions in the samples contribute to charge patterns in these hydrophilic solids.

Acknowledgment. R.F.G. is a predoctoral fellow from CNPq. The authors thank PADCT/CNPq and Pronex/Finep/MCT. This is a contribution from the Millenium Institute for Complex Materials and INCT Inomat.

Supporting Information Available: Data on weight gain and loss measurements of aluminum phosphate. This material is available free of charge via the Internet at http://pubs.acs.org.

JA900704F